Journal of Medical Ultrasonics (2019) 46:15–26
https://doi.org/10.1007/s10396-018-0899-5

ORIGINAL ARTICLE

Comparison of hypocrellin B-mediated sonodynamic responsiveness between sensitive and multidrug-resistant human gastric cancer cell lines

Yichen Liu[1] · Hong Bai[1,2] · Haiping Wang[1] · Xiaobing Wang[1] · Quanhong Liu[1] · Kun Zhang[1] · Pan Wang[1]

Received: 9 February 2018 / Accepted: 2 August 2018 / Published online: 11 October 2018

Abstract

Objectives The aim of this study was to compare the different responses to hypocrellin B (HB)-mediated sonodynamic treatment between human gastric adenocarcinoma cell line SGC7901 and SGC7901/ADR.

Methods Tumor cells in culture dishes (35-mm diameter) were exposed to planar ultrasound at an intensity of 0.5 W/cm^2 for 60 s combined with/without 2.5 μM HB. Cell viability was determined by MTT and Guava ViaCount assay. Production of reactive oxygen species (ROS) and destabilization of the mitochondrial membrane potential were assessed by flow cytometry. Apoptosis was analyzed using annexin-PE/7-amino-actinomycin D staining. The cell membrane integrity was estimated by isothiocyanate–dextran (FD500) uptake assay. Ultrastructural alterations on the membrane surface were observed by scanning electron microscopy. The membrane fluidity was also compared between the two cell lines using spectrophotometry.

Results Compared with SGC7901 cells, HB-mediated sonodynamic therapy (HB-SDT) showed higher cytotoxic in SGC7901/ADR cells at the same treatment doses. Abundant intracellular ROS, a decrease in the mitochondrial membrane potential, and an increased rate of apoptosis were detected in the SDT group of both cell lines, wherein SGC7901/ADR cells showed a much more higher rate. Cell membrane permeability was remarkably enhanced after HB-SDT application. In addition, relatively severe cell damage was observed under scanning electron microscopy after HB-SDT treatment in SGC7901/ADR cells compared with SGC7901 cells.

Conclusions These results suggest that HB-SDT could induce apoptosis in SGC7901 and SGC7901/ADR cells via production of ROS. SGC7901/ADR was found to be more sensitive to HB-SDT than SGC7901 cells under the same experimental condition. Meanwhile, a noteworthy difference in cell membrane injury between SGC7901 and SGC7901/ADR cells was detected. The decreased membrane fluidity in SGC7901/ADR cells may be one of the reasons for its increased membrane damage.

Keywords Sonodynamic therapy · Hypocrellin B · Multidrug-resistant · Gastric cancer

Introduction

Gastric cancer is a very common disease worldwide and the second most frequent cause of cancer death, affecting about one million people per year [1]. Surgical resection is the main approach of curative treatment for this highly lethal malignancy [2]. However, due to its non-specific symptoms and highly invasive characteristics, only very few patients can undergo surgery with curative intent, and the 5-year survival rates of gastric cancer patients at stage I and stage II are approximately 60% and 34%, respectively [2, 3]. Recently, neo-adjuvant chemotherapy has been widely performed to prolong survival in patients with advanced gastric cancer [4]. However, repeated chemotherapy stimulation transforms cells to the multidrug resistance (MDR)

✉ Pan Wang
wangpan@snnu.edu.cn

[1] Key Laboratory of Medicinal Resources and Natural Pharmaceutical Chemistry, Ministry of Education, National Engineering Laboratory for Resource Developing of Endangered Chinese Crude Drugs in Northwest of China, College of Life Sciences, Shaanxi Normal University, Xi'an 710062, Shaanxi, China

[2] Medical College, Xi'an Peihua University, Xi'an 710125, People's Republic of China

phenotype, which renders this approach ineffective. MDR is one of the main causes of chemotherapy failure [5]. After much chemotherapy stimulus, multidrug-resistant cells take on many different characteristics that are distinct from the parent cell, such as high expression of resistant protein, changes to the intracellular redox mechanism, and configuration and quantity changes to mitochondria and ascension of DNA repair ability. All of these changes give drug-resistant cell lines a certain resistance to other treatments such as radiotherapy and photodynamic therapy (PDT) in addition to chemotherapy. Therefore, more effective treatments are urgently needed for the treatment of gastric cancer.

An important application of low-intensity ultrasound, i.e., sonodynamic therapy (SDT), lies in the activation of certain sensitizers used in the treatment of cancer. Owing to its good penetrability, ultrasound can focus energy on tumors and kill them effectively with few side effects in normal tissue [6–8]. The direct mechanical stress and indirect chemical reactions caused by ultrasound, such as generation of reactive oxygen species (ROS), can cause lethal sonodamage, including cellular apoptosis and necrosis [9–11]. Recently, SDT has been widely investigated for its ability to damage a broad range of cancers and found to have certain curative effects. It has been reported that SDT is an effective anticancer therapy when combined with microbubbles or nanoparticles and chemotherapeutic drugs [12–14].

The physical and chemical properties of sonosensitizers directly determine the therapeutic efficacy of SDT. Hypocrellin B (HB) is a low-molecular-weight compound that belongs to the non-toxic perylenequinone family isolated from the traditional Chinese herb Hypocrella bambuase. Recently, it has been confirmed that HB can efficiently produce singlet oxygen when activated by light, and it has a strong photodynamic effect on malignant tumor cells and Gram-positive and Gram-negative bacteria [15, 16]. However, the absorption wavelength of HB (450–550 nm) limits its clinical application in photodynamic therapy (PDT) since the efficient photodynamic window is in the range of 600–900 nm. Thus, researchers have also paid attention to the sonodynamic activity of HB. Wang et al. reported that the sonodynamic action of HB significantly induced cell death of liver cancer cells and nasopharyngeal carcinoma cells via the induction of apoptosis after combined treatment with ultrasound and HB [17–20].SDT uses ultrasound that can easily penetrate deep tissue layers where some malignancies reside, thereby offsetting the major limitation of HB-based clinical application.

Our previous studies have indicated that ultrasound could cause cell membrane integrity loss, lipid peroxidation increase, and membrane morphological alterations to reverse multidrug resistance [9]. In addition, it has been reported that ultrasound can reduce the expression of ABCG2 and reverse MDR of tumors [21]. Based on the above research results, we consider that ultrasound can play a very important role in reversing MDR as a key factor in SDT. However, few studies to date have reported on the hypocrellin B-mediated sonodynamic effect on multi-resistant tumor cells, not to mention the underlying mechanism. Thus, in light of the outstanding qualities of HB as an efficient non-toxic sonosensitizer isolated from a traditional Chinese herb, HB was selected as a sensitizer to combine with ultrasound treatment to explore the anti-tumor effect of HB-SDT on SGC7901 and SGC7901/ADR cells, and to compare the different responses between SGC7901 and SGC7901/ADR cells to HB-mediated SDT by analyzing the cell survival rate, intracellular ROS production, mitochondrial damage, and cell apoptosis, etc. Given the importance of the cell membrane, one of the primary targets of ultrasound, we paid special attention to membrane damage to the two kinds of cells after sonication in order to obtain basic data on HB-mediated sonodynamic treatment to reverse MDR of tumor cells.

Materials and methods

Reagents and sonosensitizer

HB was purchased from the Institute of Chemistry, Chinese Academy of Sciences. A stock solution was made in dimethyl sulfoxide (DMSO) at a concentration of 15 mM and kept in the dark at − 20 °C until used. The chemical structure of HB is shown in Fig. 1.

Reagents including doxorubicin hydrochloride, rhodamine-123 (RHO123), 3-(4, 5-dimethylthiazol-2-yl)-2, 5-diphenyl tetrazolium bromide (MTT), 2′, 7′-dichlorodihydrofluo-rescein-diacetate (DCFH-DA), and fluorescein isothiocyanate–dextran (FD500) were purchased from Sigma-Aldrich (St. Louis, MO, USA). Guava Nexin Reagent and Guava ViaCount were obtained from Millipore Corporation (Billerica, MA, USA). Doxorubicin hydrochloride was kept as a stock solution of 2 mg/mL in sterile saline, stored at − 20 °C and thawed just prior to being used. A stock solution of FD500 was 2 mg/mL in PBS and stored at − 20 °C. The

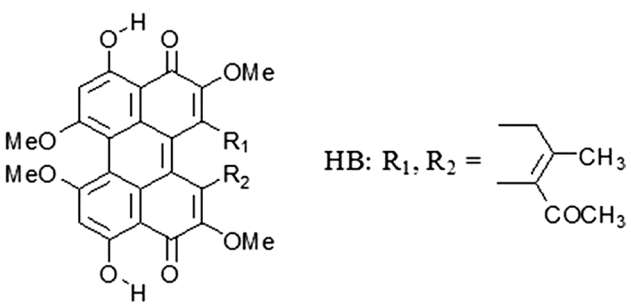

Fig. 1 The chemical structure of Hypocrellin B

work solution was 1 mg/mL diluted by PBS. Immediately prior to use, a work solution was prepared by diluting 1 µL DPH stock solution in 1 mL of 0.01 M phosphate-buffered saline (PBS) and vibrated at 25 °C until dissolved fully.

Cell culture

SGC7901 and SGC7901/ADR (DOX-resistant SGC7901 cell line) cells were obtained from Shanghai Institutes of Biological Sciences, the Chinese Academy of Sciences. Cells were cultured in RPMI-1640 medium supplemented with 10% fetal bovine serum (Hyclone, USA), 1% penicillin–streptomycin, and 1% glutamine, and then incubated at 37 °C in humidified atmosphere with a 5% CO_2 incubator. To maintain the drug-resistant phenotype, SGC7901/ADR cells were cultured in the presence of 0.7 µg/mL doxorubicin. 1 week before each experiment, SGC7901/ADR cells were cultured in a doxorubicin-free medium to avoid the influence of DOX in the treatment. All the cells in experiments were in the logarithmic phase.

Ultrasound system

For the ultrasound setup, a planar ultrasound apparatus (Fig. 2) manufactured by Sheng Xiang High Technology Co., Ltd. (China) was used in this study. The ultrasonic frequency of this apparatus was 0.84 MHz. The diameter of its planar transducer was 35 mm. The ultrasound intensity was calibrated before it was displayed in the LED screen of the apparatus. An intensity of 0.25 W/cm^2 and duration of 60 s were used for ultrasound treatment. For irradiation, the interval between transducer and cell culture plate was filled with an ultrasonic couplant to facilitate ultrasound transmission. Temperature increase inside the culture plates was measured before and after ultrasound treatment with a digital thermometer and no significant variation of temperature was detected (± 1 °C). Thus, any bio-effects observed in this study were considered to be non-thermal.

Sonodynamic therapy protocol

SGC7901 and SGC7901/ADR cells in the exponential phase were collected, resuspended in complete culture medium at the required cell density (2×10^5 cells/mL), placed in 35-mm culture dishes, and then randomly divided into four groups: (1) control group, (2) ultrasound alone group, (3) HB alone group, (4) ultrasound plus HB group (SDT). For the HB alone and SDT groups, cells were incubated with 2.5 µM HB over a 5-h drug-loading time, allowing sufficient time for cell uptake of the sonosensitizer; equivalent volumes of medium were used for the control and ultrasound groups. After drug loading, cells in the ultrasound and SDT groups were exposed to ultrasound at a frequency of 0.84 MHz and intensity of 0.5 W/cm^2 for 60 s. Every sample has three replicates.

Cytotoxicity detection by MTT assay

The cytotoxicity of HB-SDT on SGC7901 and SGC7901/ADR cells was assessed using MTT assay [22]. The HB alone and HB-mediated SDT groups were incubated with different HB doses (1.0, 2.5, 5.0 µM). After different treatment, cells were resuspended in fresh medium and cultured in a 96-well microplate at 37 °C for 24 h, and 20 µL of MTT (5.0 mg/mL, dissolved in PBS) was later added to each well and then incubated for another 4 h at 37 °C. Finally, MTT-containing medium was removed and 150 µL of DMSO was added to each well. After shaking on the platform for 10 min, the absorbance (OD) was measured using a microplate reader (Bio-Tek, ELX800, USA) at the wavelength of

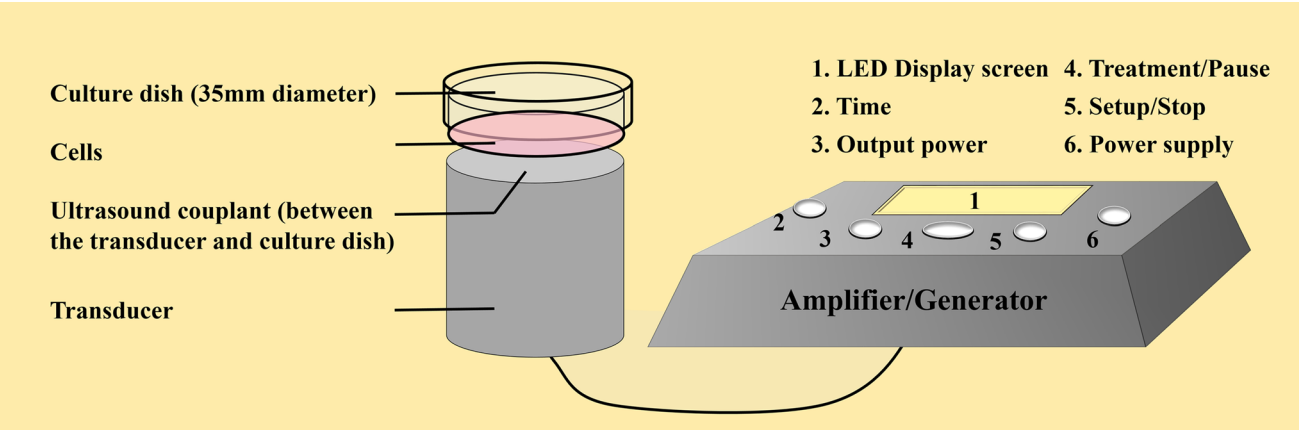

Fig. 2 Diagram of ultrasound exposure system. An ultrasound transducer with a diameter of 35 mm. The space between the transducer and cell culture plate was filled with ultrasound couplant. Culture dishes (35 mm) containing cell suspension were exposed above the transducer. The frequency of the ultrasound was 0.84 MHz

570 nm. The OD was converted to relative number of viable cells in the sample using the standard and then cell survival (%) was calculated using the following equation:

$$\text{Cell survival}\,(\%) = \frac{\text{Number of viable cells in treatment group}}{\text{Number of viable cells in control group}} \times 100\%.$$

Assessment of cell viability by flow cytometry

ViaCount assay, which distinguishes viable and non-viable cells based on differential permeability of two DNA-binding dyes in the Guava ViaCount reagent, was also employed to evaluate cell damage after different treatments. Briefly, at indicated times cells were harvested and stained with Guava ViaCount and then incubated at room temperature for 10 min; subsequently, samples were analyzed by flow cytometry (Guava EasyCyte 8HT, Millipore, Billerica, MA).

Assessment of apoptotic ratio by Annexin V-PE/7-AAD staining experiment

Annexin V-PE can detect phosphatidylserine on the external membrane of apoptotic cells and the cell-impermeant dye 7-amino-actinomycin D (7-AAD) is also used as an indicator of cell membrane integrity. After different treatments, cells were incubated for another 24 h and then harvested by trypsinization in each group. Afterwards, cells in each sample were suspended in a mixture of 100 μL of Annexin V-PE and 7-AAD binding buffer and incubated at room temperature for 30 min. Samples were then detected using flow cytometry.

Detection of intracellular ROS generation

DCFH-DA, a non-fluorescent cell-permeant compound, is cleaved by endogenous esterases within the cell and the de-esterified product can be converted into the fluorescent compound dichlorofluorescein (DCF) upon oxidation by intracellular ROS. Therefore, we studied production of ROS by measuring the fluorescence intensity of DCF. Briefly, cells were incubated with 4 μM DCHF-DA at 37 °C for 30 min prior to treatment. After 1 h, cells were harvested by trypsinization in each group and subjected to flow cytometry analysis. Histograms were analyzed using FCS Express version 3 software.

Measurement of mitochondrial membrane potential

Changes in MMP were measured by uptake of fluorescent cationic rhodamine123 (RHO123) in mitochondria with an intact membrane potential [23]. Once the MMP is lost, it cannot provide enough potential gradient for RHO123 to be absorbed and retained in the mitochondria. At *2 h* after different treatments, cells were harvested and washed with PBS twice, and then incubated with 1 μg/mL RHO123 in serum-free RPMI-1640 medium at 37 °C in the dark for 30 min. Afterwards, cells were harvested, excess dye was washed away, and cells resuspended with PBS were immediately examined by flow cytometry. The data analysis was performed using FCS Express V3 software.

Detection of intracellular drug accumulation

To test the absorptive capacity of SGC7901 and SGC7901/ADR cells to anticancer drug HB, we detected the intracellular accumulation of HB before ultrasound. In short, after cells were incubated in serum-free RPMI-1640 medium containing HB for 5 h, cells were harvested and washed in phosphate-buffered saline and then immediately analyzed by flow cytometry.

Detection of cell membrane integrity

To measure the changes in membrane permeability induced by HB-SDT, FD500-uptake assay was performed. FD500 is the conjugate of fluorescein FITC and dextran that cannot freely penetrate the cell membrane. But FD500 may enter the cells once membrane permeability is enhanced after some special treatment, after which we can detect the change in membrane permeability from the intracellular fluorescent signal [9]. To measure changes in membrane permeability induced by different treatments, SGC7901 cells and SGC7901/ADR cells were treated with the different means in the presence of 1 mg/mL of FD500. After ultrasonic treatment, cells were immediately washed with PBS, after which the FD500-positive cells were quantified by flow cytometry.

Scanning electron microscope (SEM) observation

Immediately after different treatments, cells were fixed in 2.5% glutaraldehyde in 0.1 mol of PBS (pH 7.2), washed with PBS, dehydrated with graded alcohol, displaced, dried at the critical point, gold evaporated, and observed under a scanning electron microscope.

Fluorescence polarization for membrane fluidity

DPH is a hydrophobic molecule. It cannot be detected by fluorescence in aqueous solution because the molecular folding is in cis conformation. However, DPH can enter the membrane lipid area when it is mixed with the cell suspensions. In a hydrophobic environment, DPH emits fluorescence since the molecule becomes unfolded, resulting in DPH converting from cis conformation to trans conformation.

Immediately after ultrasound treatment, cells were harvested and 2 mL of DPH work solution was added. After incubation for 30 min at 37 °C, the cell suspensions were washed with PBS at 25 °C and resuspended in 4 mL of PBS.

Cell suspensions containing no DPH were similarly assessed to check light scattering. Analyses were performed with a fluorescence lifetime spectrometer (PTI, USA) equipped with two polarizers that allowed instantaneous measurement of the vertical and horizontal fluorescence. The samples were excited with polarized light (365 nm). Emission (430 nm) was measured to get the degree of fluorescence polarization (Pr). Membrane fluidity (LFU) = $0.5 - P/P^2$.

Statistical analysis

Data are presented as mean ± SD. Differences among the groups were assessed with a one-way analysis of variance. A p value < 0.05 was considered to indicate statistical significance, and $p < 0.01$, high significance.

Results

Cytotoxicity of HB-SDT in SGC7901 cells and SGC7901/ADR cells

Cytotoxicity in SGC7901 and SGC7901/ADR cells was tested at 24 h after treatment. Figure 3a shows that no inhibitory effect was observed in the HB alone groups (1.0 μM, 2.5 μM, 5 μM) for both SCG-7901 and SCG-7901/ADR cells. The results in Fig. 3b show that, in comparison to SGC7901 cells, the viability of SGC7901/ADR cells was clearly lower when exposed to the same intensity of ultrasound. For both cell types, 0.25 W/cm^2 did not show any statistical difference compared with the control group. Meanwhile, 0.5 W/cm^2 showed a relatively appropriate cell viability rate at about 87.24% and 69.72% for SGC7901 and SGC7901/ADR cells, respectively. For SGC7901 cells, 0.5 W/cm^2 ultrasound alone did not show significant cytotoxicity, but when we combined HB and ultrasound, the cell viability significantly declined to 63.67% ($p > 0.05$) and 41.06% ($p < 0.05$), respectively, with HB doses of 2.5 μM and 5.0 μM. The cytotoxicity in SGC7901/ADR cells when mediated by HB-SDT was also significant. When treated by SDT with 2.5 μM or 5 μM HB, the cell survival rate declined to 44.56% ($p < 0.05$) and 21.28% ($p < 0.01$), respectively (Fig. 3c). For subsequent experiments, we selected 2.5 μM HB concentration and 0.5 W/cm^2 in SDT treatment.

To further confirm the results of MTT assay, Guava ViaCount assay was performed. The result in Fig. 3d, e indicates that for SGC7901 cells, cell viability was 94.20%

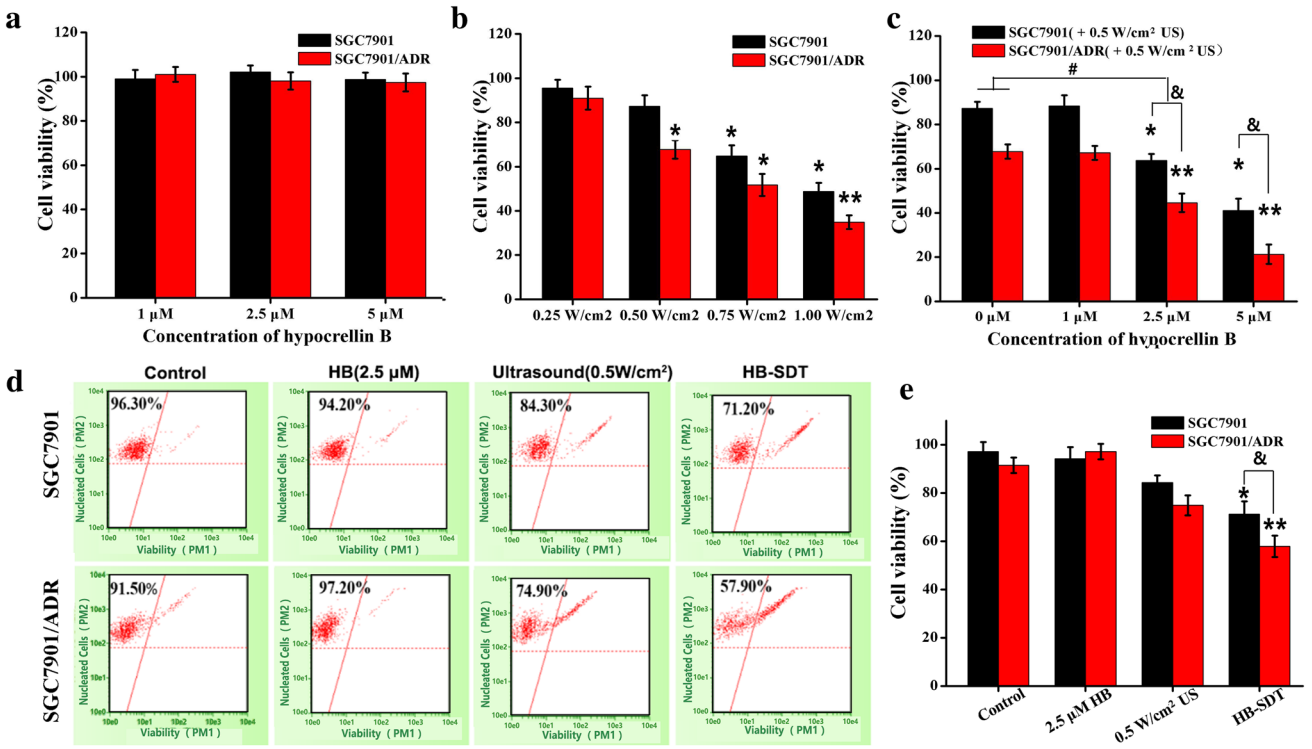

Fig. 3 The cytotoxic effect determined by MTT assay 24 h after treatment. **a** Cytotoxic effect of HB alone. **b** Cell viability of both cells under ultrasound irradiation at intensities ranging from 0.25–0.75 W/cm^2. **c** Cell viability under HB-SDT treatment. **d** Analysis of cell viability by Guava ViaCount assay. Cells were analyzed 24 h post-different treatments. **e** Quantitative data of ViaCount assay. Error bars represent the SD from three independent experiments. *$p < 0.05$ versus control, **$p < 0.01$ versus control, &$p < 0.05$ SGC7901 cell group versus SGC7901/ADR cell group

in the 2.5 μM HB group, and the cell survival rate declined to 84.30% and 71.20% in the 0.5 W/cm^2 ultrasound treatment and SDT groups, respectively. For SCG-7901/ADR cells, 2.5 μM HB also did not show any obvious cytotoxicity, whereas ultrasound and SDT treatment, respectively, caused 25.10% and 42.10% ($p < 0.05$) cell viability loss. This result was approximately consistent with the results obtained from MTT assay.

Induction of apoptosis by HB-SDT

The apoptosis rate was analyzed with Annexin V-PE and 7-ADD staining 24 h after treatment. According to the product specification, Annexin V positive staining is an indicator of both early apoptosis and later apoptosis, whereas 7-AAD labels only cell death representing necrosis and cell debris. As indicated in Fig. 4a, b, in the HB alone group, the proportion of apoptosis was 2.85% and 3.30% ($p > 0.05$) for SGC7901 and SGC7901/ADR cells, respectively. In the ultrasound alone groups, the ratio of apoptosis increased to 20.90% ($p > 0.05$) and 22.07% ($p < 0.05$) under the intensity of 0.5 W/cm^2 for 60 s for SGC7901 and SGC7901/ADR cells, respectively. When ultrasound and HB were combined, the apoptotic rates in SGC7901 and SGC7901/ADR cells enhanced to 32.93% ($p < 0.05$) and 55.23% ($p < 0.01$), respectively.

Measurement of ROS production

Recently, it has been confirmed that HB can efficiently produce singlet oxygen when activated by light and elicit a significant anti-tumor effect [19, 24]. ROS may be one of the key factors in SDT-induced cell damage. Therefore, intracellular ROS was detected by DCFH-DA staining immediately after treatment to explore whether ROS was involved in HB-SDT or not. Intracellular ROS formation was monitored after the different treatments by measuring the conversion of non-fluorescent DCFH-DA to fluorescent DCF using flow cytometry. As indicated in Fig. 5, 1 h after treatments, compared with control, no cells in the HB alone groups had higher DCF fluorescence in the two cell lines, but 26.45% and 43.45% ($p < 0.05$) of cells in the HB-SDT groups displayed higher DCF fluorescence in SGC7901 and SGC7901/ADR cells, respectively.

MMP changes induced by HB-SDT

RHO123 staining was adopted to evaluate MMP changes induced by HB-SDT. The mean fluorescence intensity of RHO123 was used as an indicator that is directly proportional to MMP. The results illustrated in Fig. 6a, b showed that compared with control, HB-SDT could cause obvious MMP change in both SGC7901 and SGC7901/ADR cells at the rate of *49.81% and 69.65%* ($p < 0.01$), respectively. In contrast, HB alone could not produce obvious MMP changes in the above two cell lines. Moreover, we found that SGC7901/ADR cells had more RHO123 fluorescence when compared with SGC7901 cells under the same processing conditions in the ultrasound groups.

Measurement of the HB accumulation in cells

To detect the intracellular drug accumulation before ultrasound treatment, we monitored the fluorescence intensity of HB by flow cytometry. Statistics in Fig. 7 show that after incubation for 5 h, the dosage of HB in SGC7901 cells was almost at the same level as SGC7901/ADR cells when compared to each of the control groups.

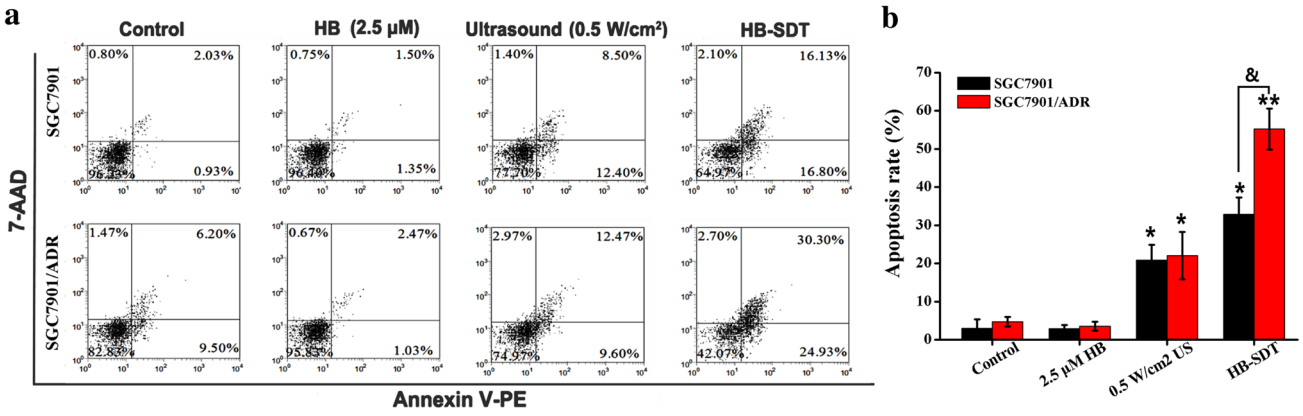

Fig. 4 Analysis of cell apoptosis by Guava Apoptosis assay. **a** Cells were analyzed 24 h post-different treatments. **b** Quantitative data of apoptosis assay. Error bars represent the SD from three independent experiments. *$p < 0.05$ versus control, **$p < 0.01$ versus control, &$p < 0.05$ SGC7901 cell group versus SGC7901/ADR cell group

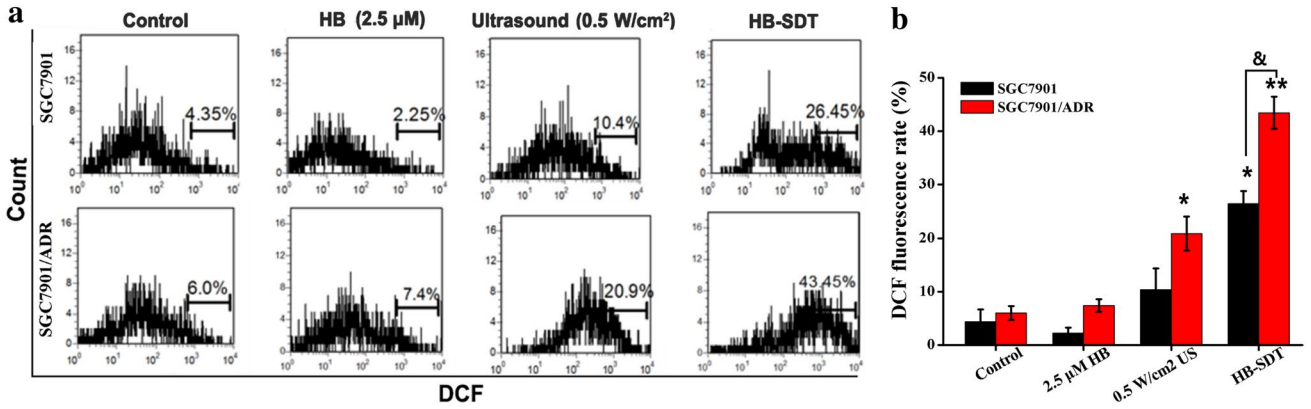

Fig. 5 Measurement of intracellular ROS generation in cells detected by flow cytometry. **a** Cells were analyzed 1 h post-different treatments. **b** Quantitative data of intracellular ROS generation. Error bars represent the SD from three independent experiments. $*p<0.05$ versus control, $**p<0.01$ versus control, $\&p<0.05$ SGC7901 cell group versus SGC7901/ADR cell group

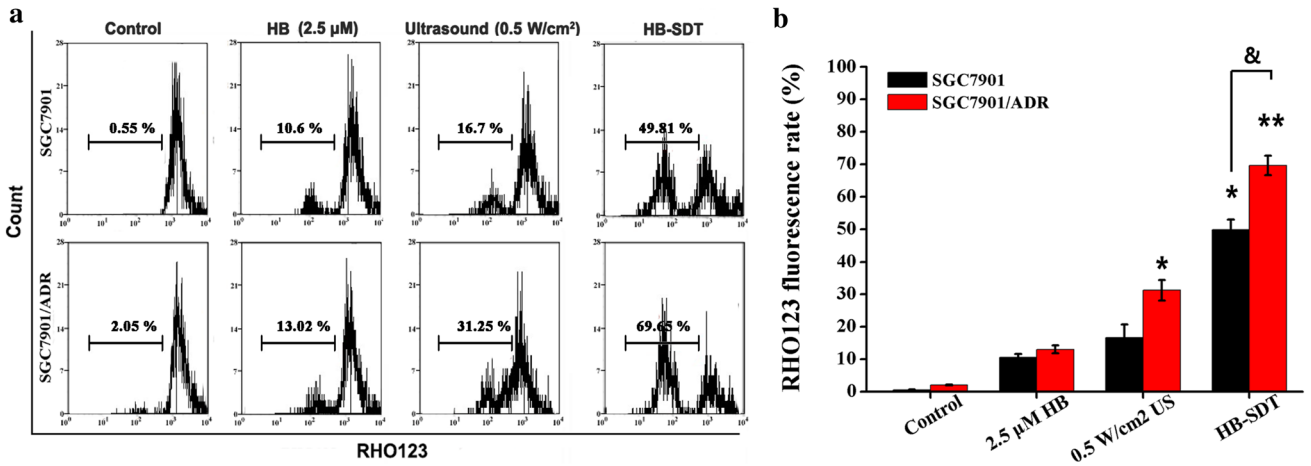

Fig. 6 Changes in mitochondrial membrane potential detected by flow cytometry. **a** Cells were analyzed 24 h post-different treatments. **b** Quantitative data on drop rate of mitochondrial membrane potential. Error bars represent the SD from three independent experiments. $*p<0.05$ versus control, $**p<0.01$ versus control, $\&p<0.05$ SGC7901 cell group versus SGC7901/ADR cell group

HB-SDT-induced membrane permeability change

Cell membrane integrity could be evaluated by FD500-uptake assay. Studies have shown that FD500 does not stick on the cell membrane and rarely enters dead cells. Thus, the uptake of FD500 can be a credible sign that reflects the membrane permeability. Data in Fig. 8 show that the proportion of SGC7901/ADR cells exhibiting high fluorescence intensities of FD500 increased to 52.80% in the HB-SDT group. On the other hand, it was only 35.73% in SGC7901 cells. The result might suggest that injury of the cell membrane in SGC7901/ADR cells was more serious than that in SGC7901 cells under the same treatment conditions.

Ultrasound-induced morphological changes

The effect of ultrasound was morphologically observed under SEM (Fig. 8). As shown in Fig. 9, SGC7901 cells in the control group appeared to show their normal shape with an intact membrane and abundant microvilli, with its pseudopodia being at full stretch, tightly sticking on the cover glass. Cells treated by HB-SDT and ultrasound were not significantly different when compared with control cells, while SGC7901/ADR cells (Fig. 9) after the same treatment showed obvious morphological changes including marked shrinkage and the disclosure of content. This might directly reflect that cell membrane damage in SGC7901/ADR cells was much more severe.

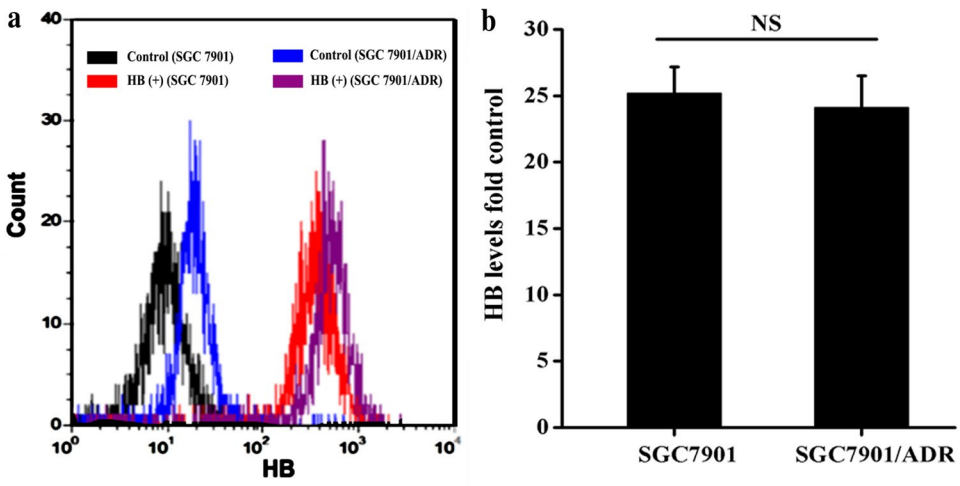

Fig. 7 The fluorescence of HB in cells. **a** Cells were analyzed 5 h post-incubation. **b** Quantitative data of HB levels fold control. Error bars represent the SD from three independent experiments. *$p < 0.05$ SGC7901 cell group versus SGC7901/ADR cell group

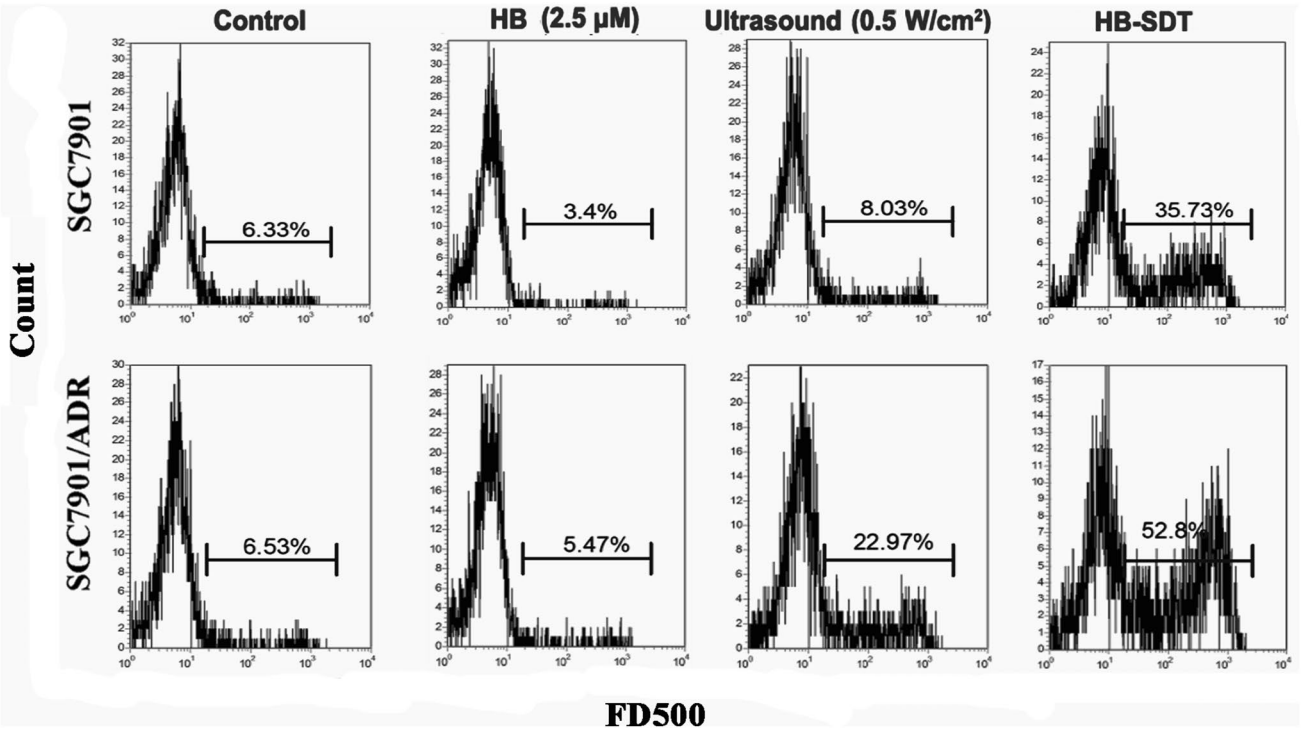

Fig. 8 Changes in cell membrane permeability detected by flow cytometry

Analysis of membrane fluidity

It has been reported that the plasma membrane is the primary target in ultrasound and the membrane fluidity affects the function of the cell membrane to a large extent, such as carrier-mediated transport, the properties of certain membrane-bound enzymes, and cell growth. Different cell membranes exhibit different sensitivity to sonication [8]. Based on these, we detected the membrane fluidity of these two cell lines by fluorescence polarization. As displayed in Fig. 10a, b, the cell membrane fluidity of SGC7901/ADR cells was significantly lower compared with SGC7901 cells.

Discussion

It is well known that MDR is one of the primary obstacles to successful cancer chemotherapy [5]. Although many MDR-reversing agents have been found to overcome

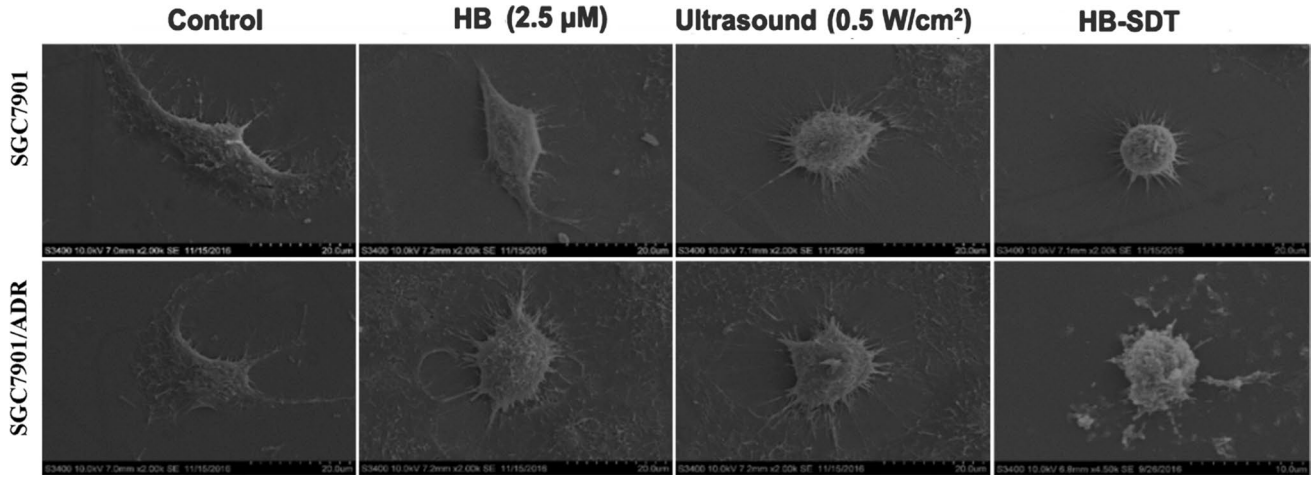

Fig. 9 SEM observation of SGC7901 and SGC7901/ADR cells after treatment with HB-SDT

drug resistance in some studies, they may also expose the patient to undesired effects or affect the efficiency of the accompanying anticancer drugs [25]. These limitations have spurred efforts to seek more effective methods to reverse MDR. Studies have shown that sonodynamic therapy, similar to photodynamic therapy, can kill target cells via the production of cytotoxic ROS after ultrasound activates a sonosensitizer [26]. HB, a natural sensitizer derived from traditional Chinese medicine, is a great ROS generator after the activation of photoenergy or ultrasound wave, thus inducing cell death of target cells [19]. Given that ultrasound could dramatically cause cytotoxicity and contribute to reversing multidrug resistance, as reported by many scholars [9], we initially carried out a series of fundamental investigations to make a comparison between SGC7901/ADR and its parent counterpart SGC7901 cells after HB-SDT treatment to provide more information for MDR reversal in human gastric cancer.

First, cell death information after SDT treatment was evaluated by MTT and Guava ViaCount assay. The results obtained from MTT and ViaCount assay (Fig. 3) suggested that HB-SDT could significantly kill both SGC7901 cells and SGC7901/ADR cells. Meanwhile, compared with SGC7901 cells, SGC7901/ADR cells were more sensitive to ultrasound and SDT treatment, which was consistent with previous research [9].

Apoptosis appears to be a common mechanism of biological activity for cytotoxic agents employed in tumor therapy. To date, many studies have documented the sonodynamic induction of apoptosis in a variety of cancer cell types with an array of different sensitizers [27, 28]. We conducted experiments to determine whether the inhibition of cell viability observed after HB-SDT was the result of induction of cell apoptosis. The result of Annexin V-PE/7-AAD assay in our study demonstrated changes in cell apoptosis

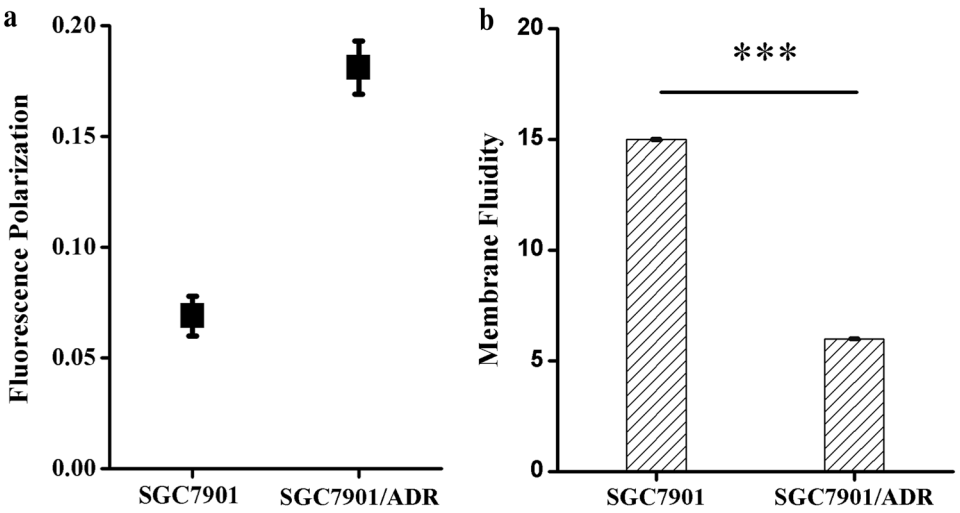

Fig. 10 Membrane fluidity of SGC7901 and SGC7901/ADR cells. **a** The degree of fluorescence polarization (Pr) **b** membrane fluidity (LFU). ***The statistical significance between SGC7901 and SGC7901/ADR cells. Error bars represent the SD from three independent experiments

after HB-SDT. SGC7901/ADR cells also showed a more significant effect of HB-SDT on apoptosis.

As described by other researchers, ROS may be one of the key factors in SDT-induced cell damage [29, 30]. Excessive ROS may damage lipids, proteins, and DNA, and cause mitochondrial dysfunction, deregulation of ion balance, and loss of membrane integrity [31]. In our study, substantial enhancement of ROS was detected 1 h after HB-SDT. In addition, the yield of ROS triggered by the combination of HB and ultrasound in SGC7901/ADR cells was about 1.5-fold that in SGC7901 cells, indicating that SGC7901/ADR cells showed a greater response to HB-SDT than SGC7901 cells.

Previous investigations showed that mitochondria, as the major energy generators in cells, play a vital role in cell apoptosis induced by many stimuli [32]. In addition, previous research has indicated that HB can localize in the mitochondria [33]. Hence, we speculated that the mitochondria may be a lesion site of HB-SDT. Subsequently, we monitored an initial MMP drop in cells after HB-SDT, indicating disaggregation of MMP and functional impairment of mitochondria after HB-SDT treatment (Fig. 6). We also found that the collapse of mitochondria membrane potential in SGC7901/ADR cells was more obvious, which may manifest as SGC7901/ADR cells being more sensitive to the mitochondria damage caused by HB-SDT.

As SDT is a synergistic effect of sonosensitizers and ultrasound, the accumulation of sonosensitizers in tumor cells affects the SDT efficiency directly. To explore whether the different manifestations of SDT treatment on SGC7901 and SGC7901/ADR cells were induced by intracellular HB dose, the HB concentration in different cell lines was detected by flow cytometry. The results in Fig. 7 indicated that there was nearly no difference in HB uptake between SGC7901 and SGC7901/ADR cells. So another mechanism may be involved in the different sensitivities to HB-SDT in these two kinds of cells.

The cell damage effect of ultrasound irradiation was specially examined from the view of membrane damage. As the first barrier, the plasma membrane plays an important role in the defense against cell damage from various harmful stimuli and it has been considered to be one of the critical targets for ultrasound-induced action [34]. Alteration of the plasma membrane structure has been recognized as a significant effect associated with cytotoxic damage and examination of the effect may consequently provide important information on both the mechanism of ultrasound and other factors [35]. In this study, some related changes in the plasma membrane were investigated, with an emphasis on changes in the cell membrane integrity and its ultrastructural changes. The result obtained from FD500-uptake assay suggested that the membrane damage to SGC7901/ADR cells was much more serious than that to SGC7901 cells under the same HB-SDT experimental condition. The data suggested that ultrasound could cause a loss of cell membrane integrity, which might be due to the alterations in the structures and function of the plasma membrane post-ultrasound exposure, which also showed that cell membrane morphology damage in SGC7901/ADR cells was much more serious compared to SGC7901 cells under the same ultrasound conditions. The remarkable alterations, including decreased microvilli and obvious structural changes on the cell surface post-ultrasound treatment, may affect membrane functions, eventually leading to cell dysfunction and even death. Thus, the results of morphological evaluation were consistent with the tendency of cell viability demonstrated above.

Previous research has shown that MDR is one of the major obstacles in the effective treatment of cancer. Abundant evidence has shown that the majority of MDR may be due to the overexpression of P-glycoprotein (P-gp) proteins. P-gp confers MDR by acting as an ATP-dependent pump, which actively effluxes drugs out of cancer cells. Kong et al. demonstrated that overexpression of P-gp may be one of the main reasons that MCF-7/ADR cells are resistant to anticancer drugs, and they detected decreased expression of P-gp when they tried to reverse multidrug resistance in MCF-7/ADR cells using *Curcuma wenyujin* and *Chrysanthemum indicum* [36]. Research has shown that overexpression of P-gp leads to higher membrane rigidity for multidrug-resistant cells [37–39] and the level of membrane rigidity is inversely proportional to membrane fluidity [40]. Thus, we speculate that the level of membrane fluidity in SGC7901/ADR cells may be lower owing to overexpression of P-gp. To confirm the hypothesis, we conducted an experiment to detect the membrane fluidity by fluorescence polarization (Fig. 10). The data suggested that the level of membrane fluidity in SGC7901/ADR cells was lower than that in SGC7901 cells. Hassan et al. found that doxorubicin-resistant uterine sarcoma MES-SA/DX5 cells suffered from unfavorable conditions for membrane repair post-acoustic exposure owing to a higher level of membrane rigidity induced by overexpression of P-gp [38]. Jia et al. reported that MCF-7/ADR cells were more sensitive to ultrasound exposure than MCF-7 cells under the same experimental conditions. The decreased membrane fluidity in MCF-7/ADR cells may be one of the reasons for its increased membrane damage [9]. Herein, the decrease in membrane fluidity will increase the membrane tension. The increased membrane tension, on the one hand, may reduce the membrane permeability and contribute to lowering the efficiency of intracellular drug accumulation. However, on the other hand, the increased membrane tension inhibits membrane repair when exposed to US and SDT, which may induce SGC7901/ADR cells to become more sensitive to US and SDT than SGC7901 cells. Hence, we hypothesis that a low level of membrane fluidity may be one of the reasons why SGC7901/ADR cells

showed a severe loss of cell viability, higher apoptotic rate, increased uptake of FD500, and more serious morphological damage when treated with HB-SDT. However, whether overexpression of P-gp contributed to the low level of membrane fluidity needs to be further confirmed. Also, the changes in membrane fluidity of both cells before/after ultrasound irradiation as well as HB-SDT treatment need to be investigated in detail in follow-up research.

Conclusions

In summary, we performed assessments of the sonodynamic effects of HB on human gastric cancer cells. The results suggested that SGC7901/ADR cells were much more sensitive to HB-mediated sonodynamic treatment than SGC7901 cells, while the dose of HB in the two cell lines showed almost no differences. Furthermore, fluorescence polarization experimental results showed that SGC7901/ADR cells had lower membrane fluidity than SGC7901 cells, which we suspected might contribute to its susceptibility to HB-mediated sonodynamic treatment. The current experimental results may lead to new design ideas to reverse multidrug resistance in human gastric cancer SGC7901/ADR cells.

Acknowledgements This work was supported by the National Natural Science Foundation of China (Grant No. 81872497), the Fundamental Research Funds for the Central Universities (No. GK201602003, 2016TS056), and the Natural Science Foundation of Shaanxi Province (No. 2017JM8004).

Compliance with ethical standards

Conflict of interest The authors declare that they have no conflicts of interest.

Ethical statements All procedures followed were in accordance with the ethical standards of the responsible committee on human experimentation (institutional and national) and with the Helsinki Declaration of 1964 and later versions.

References

1. Hartgrink HH, Jansen EP, van Grieken NC, et al. Gastric cancer. Lancet. 2009;374:477–90.
2. Mu J, Liu T, Jiang L, et al. The traditional chinese medicine baicalein potently inhibits gastric cancer cells. J Cancer. 2016;7:453–61.
3. Parkin DM, Pisani P, Ferlay MJ. Global cancer statistics. CA Cancer J Clin. 1999;49:33–64.
4. Wang P, Li Z, Liu H, et al. MicroRNA-126 increases chemosensitivity in drug-resistant gastric cancer cells by targeting EZH2. Biochem Biophys Res Commun. 2016;479:91–6.
5. Sun W, Lv C, Zhu T, et al. Ophiobolin-O reverses adriamycin resistance via cell cycle arrest and apoptosis sensitization in adriamycin-resistant human breast carcinoma (MCF-7/ADR) cells. Mar Drugs. 2013;11:4570–84.
6. Li C, Zhang K, Wang P, et al. Sonodynamic antitumor effect of a novel sonosensitizer on S180 solid tumor. Biopharm Drug Dispos. 2014;35:50–9.
7. Li Q, Wang X, Wang P, et al. Efficacy of chlorin e6-mediated sono-photodynamic therapy on 4T1 cells. Cancer Biother Radiopharm. 2014;29:42–52.
8. Li Y, Wang P, Wang X, et al. Involvement of mitochondrial and reactive oxygen species in the sonodynamic toxicity of chlorin e6 in human leukemia K562 cells. Ultrasound Med Biol. 2014;40:990–1000.
9. Jia Y, Yuan W, Zhang K, et al. Comparison of cell membrane damage induced by the therapeutic ultrasound on human breast cancer MCF-7 and MCF-7/ADR cells. Ultrason Sonochem. 2015;26:128–35.
10. Su X, Chen Y, Wang X, et al. PpIX induces mitochondria-related apoptosis in murine leukemia L1210 cells. Drug Chem Toxicol. 2014;37:348–56.
11. Wang H, Wang X, Wang P, et al. Ultrasound enhances the efficacy of chlorin E6-mediated photodynamic therapy in MDA-MB-231 cells. Ultrasound Med Biol. 2013;39:1713–24.
12. Shen S, Wu L, Liu J, et al. Core-shell structured Fe_3O_4@TiO_2-doxorubicin nanoparticles for targeted chemo-sonodynamic therapy of cancer. Int J Pharm. 2015;486:380–8.
13. Wang H, Wang P, Li L, et al. Microbubbles enhance the antitumor effects of sinoporphyrin sodium mediated sonodynamic therapy both in vitro and in vivo. Int J Biol Sci. 2015;11:1401–9.
14. Yoshida T, Kondo T, Ogawa R, et al. Combination of doxorubicin and low-intensity ultrasound causes a synergistic enhancement in cell killing and an additive enhancement in apoptosis induction in human lymphoma U937 cells. Cancer Chemother Pharmacol. 2008;61:559–67.
15. Jiang Y, Leung AW, Wang X, et al. Effect of photodynamic therapy with hypocrellin B on apoptosis, adhesion, and migration of cancer cells. Int J Radiat Biol. 2014;90:575–9.
16. Jiang Y, Xia X, Leung AW, et al. Apoptosis of breast cancer cells induced by hypocrellin B under light-emitting diode irradiation. Photodiagnosis Photodyn Ther. 2012;9:337–43.
17. Jiang Y, Leung AW, Wang X, et al. Inactivation of Staphylococcus aureusby photodynamic action of hypocrellin B. Photodiagnosis Photodyn Ther. 2013;10:600–6.
18. Wang P, Xu CS, Xu J, et al. Hypocrellin B enhances ultrasound-induced cell death of nasopharyngeal carcinoma cells. Ultrasound Med Biol. 2010;36:336–42.
19. Wang X, Leung AW, Jiang Y, et al. Hypocrellin B-mediated sonodynamic action induces apoptosis of hepatocellular carcinoma cells. Ultrasonics. 2012;52:543–6.
20. Wang X, Ip M, Leung AW, et al. Sonodynamic action of hypocrellin B on methicillin-resistant Staphylococcus aureus. Ultrasonics. 2016;65:137–44.
21. Bai M, Shen M, Teng Y, et al. Enhanced therapeutic effect of Adriamycin on multidrug resistant breast cancer by the ABCG2-siRNA loaded polymeric nanoparticles assisted with ultrasound. Oncotarget. 2015;6:43779–90.
22. Wang X, Hu J, Zhang S, et al. Analysis of the in vivo and in vitro effects of photodynamic therapy on breast cancer by using a sensitizer, sinoporphyrin sodium. Theranostics. 2015;7:772–86.
23. Wang ZB, Liu YQ, Zhang Y, et al. Reactive oxygen species, but not mitochondrial membrane potential, is associated with radiation-induced apoptosis of AHH-1 human lymphoblastoid cells. Cell Biol Int. 2007;31:1353–8.
24. Wang X, Leung AW, Hua H, et al. Sonodynamic action of hypocrellin B on biofilm-producing Staphylococcus epidermidis in planktonic condition. J Acoust Soc Am. 2015;138:2548–53.

25. Krishna R, Mayer LD. Multidrug resistance (MDR) in cancer. Mechanisms, reversal using modulators of MDR and the role of MDR modulators in influencing the pharmacokinetics of anticancer drugs. Eur J Pharm Sci. 2000;11:265–83.
26. Wang H, Wang X, Zhang S, et al. Sinoporphyrin sodium, a novel sensitizer, triggers mitochondrial-dependent apoptosis in ECA-109 cells via production of reactive oxygen species. Int J Nanomed. 2014;2014:3077–90.
27. Escoffre JM, Piron J, Novell A, et al. Doxorubicin delivery into tumor cells with ultrasound and microbubbles. Mol Pharm. 2011;8:799–806.
28. Tang W, Fan W, Liu Q, et al. The role of p53 in the response of tumor cells to sonodynamic therapy in vitro. Ultrasonics. 2011;51:777–85.
29. Costley D, Mc Ewan C, Fowley C, et al. Treating cancer with sonodynamic therapy: a review. Int J Hyperthermia. 2015;31:107–17.
30. Zheng X, Wu J, Shao Q, et al. Apoptosis of THP-1 macrophages induced by pseudohypericin-mediated sonodynamic therapy through the mitochondria-caspase pathway. Cell Physiol Biochem. 2016;38:545–57.
31. Yumita N, Iwase Y, Nishi K, et al. Involvement of reactive oxygen species in sonodynamically induced apoptosis using a novel porphyrin derivative. Theranostics. 2012;2:880–8.
32. Li Q, Liu Q, Wang P, et al. The effects of Ce6-mediated sonophotodynamic therapy on cell migration, apoptosis and autophagy in mouse mammary 4T1 cell line. Ultrasonics. 2014;54:981–9.
33. Wang X, Luo J, Leung AW, et al. Hypocrellin B in hepatocellular carcinoma cells: subcellular localization and sonodynamic damage. Int J Radiat Biol. 2015;91:1–22.
34. Miller DL, Dou C. Membrane damage thresholds for pulsed or continuous ultrasound in phagocytic cells loaded with contrast agent gas bodies. Ultrasound Med Biol. 2004;30:405–11.
35. Hao Q, Liu Q, Wang X, et al. Membrane damage effect of therapeutic ultrasound on Ehrlich ascitic tumor cells. Cancer Biother Radiopharm. 2009;24:41–8.
36. Yang L, Wei DD, Chen Z, et al. Reversal of multidrug resistance in human breast cancer cells by *Curcuma wenyujin* and *Chrysanthemum indicum*. Phytomedicine. 2011;18:710–8.
37. Boutin C, Roche Y, Millot C, et al. High heterogeneity of plasma membrane microfluidity in multidrug-resistant cancer cells. J Biomed Opt. 2009;14:034030.
38. Hassan MA, Furusawa Y, Minemura M, et al. Ultrasound-induced new cellular mechanism involved in drug resistance. PLoS One. 2012;7:e48291.
39. Wang E, Lee MD, Dunn KW. Lysosomal accumulation of drugs in drug-sensitive MES-SA but not multidrug-resistant MES-SA/Dx5 uterine sarcoma cells. J Cell Physiol. 2000;184:263–74.
40. Tang W, Liu Q, Wang X, et al. Membrane fluidity altering and enzyme inactivating in sarcoma 180 cells post the exposure to sonoactivated hematoporphyrin in vitro. Ultrasonics. 2008;48:66–73.